Digest Journal of Nanomaterials and Biostructures Vol. 16, No. 4, October-December 2021, p. 1219-1226

Synthesis and study of the optical and structural properties of Au and Ag nanoparticles by pulsed laser ablation (PLAL) technique

A. A. Kamil*, N. A. Bakr, T. H. Mubarak, J. Al-Zanganawee
Department of Physics, College of Science, University of Diyala, Diyala, Iraq

Gold and silver nanoparticles (NPs) were synthesized by Q-switched (Nd:YAG) Pulsed Laser Ablation in Liquid (PLAL). The colloidal solutions are prepared separately using wavelength between 532-1064 nm pulsed laser ablation of gold and silver targets that are immersed in distilled water. The absorption spectra and color variations of gold and silver NPs at six different laser pulses (150, 250,350, 450, 550, 650 pulses) were investigated. UV–Vis spectroscopy test displayed bands ranged between 520 nm for gold and 404-410 nm for silver. TEM revealed a spherical shape of gold and a semi-spherical shape of silver NPs with an average sizes of (7.95 nm to 11.36 nm) and (15.62 nm to 20.49 nm) from two pulses (150 and 650), respectively. At all numbers of pulses applied, XRD showed a cubic crystalline structure of Au particles, as well as the creation of a pure cubic crystal structure of Ag particles and another cubic crystal structure attributed to AgO particles.

(Received May 18, 2021; Accepted October 5, 2021)

Keywords: Pulsed laser ablation PLAL, AuNps, AgNps, Spherical shape, Optical properties

1. Introduction

Noble metal NPs such as silver (Ag) and gold (Au) are the most appealing elements due to their novel electrical, optical, physical, chemical and magnetic properties [1,2]. Both Au and Ag NPs have a plasmonic effect due to the dispersion and absorption of photons. Nanoparticles produced by PLAL are suitable for biomedical and physical applications. Therefore, this feature of ablation makes it a unique technology for the production of nanoparticles [3]. PLAL is slowly but steadily gaining popularity as a chemically simple and safe process with high product purity [4-6]. Moreover, the procedure can be carried out at room temperature and pressure and product structures and properties can be easily monitored by changing the experimental conditions like the laser parameters, solutions, external environment and target material [7].

Au-NPs and Ag-NPs are not sensitive to physical factors such as air, light, electronic properties related to size, good conductivity, chemical stability, magnetic properties [8,9]. When the size of Au-NPs and Ag-NPs is less than the wavelength ($R<<\lambda$) of the incident light, the physical and chemical properties of these NPs become more appropriate [10]. The presence of an incident beam (electromagnetic field) at a specific wavelength can cause free electrons to be in a state of resonance through a particle known as Surface Plasmon Resonance (SPR) [10,11]. Because of their broad applications in the preparation of other nanoparticles such as metals, oxides, alloys, semiconductors, and noble metals, the physical method (top-down) was used in this study to synthesize Au-NPs and Ag-NPs [12,13].

One of the top-down methods is PLAL which is based on the laser pulses focused on the bulk target. Through the emission of shockwaves, the bulk target absorbs and creates a plasma plume that rapidly spreads into the surrounding solvent medium. Finally, within nano- to microseconds, the target cools down, extinguishes, and decomposes. Subsequently, the atomized material that has been extracted from the target can interact with the solvent and solute species, resulting in nanoparticle nucleation, growth, and formation [14]. It has been demonstrated via realistic experiments that adjusting different parameters such as the wavelength of the laser, the duration of the pulse, and the pH of the solution can regulate the size of the resulting nanoparticles [15]. The aim of this study was to synthesize nanoparticles from gold and silver targets by laser

* Corresponding author: asaad181162@yahoo.com

ablation method and investigate their structural and optical properties for optical devices and gas sensors applications.

2. Experimental Method

2.1. Synthesis of gold and silver NPs

Pulsed Laser Ablation in Liquid (PLAL) was used to synthesize Au-NPs and Ag-NPs. Pure gold and silver plates were cleaned by ethanol to eliminate the foreign organic substances as a result of washing with distilled water. To avoid liquid failure, the plates were placed in a beaker containing 5 ml of distilled water, and the targets were placed 6 cm from the focal point [16]. The system includes a source of laser Q-switched Nd: YAG (HUAFEI, China) with a wavelength between 532-1064 nm, 1Hz frequency and 520 MJ laser energy. The colloidal solution becomes red for Au-NPs and yellow for Ag-NPs after the process of laser ablation. The absorption spectra for the prepared samples and SPR was measured by using UV–Vis spectrometer (UV-1800, Shimadzu , Japan). The crystallographic structure was carried out by using X-ray analysis (XRD Phillips Xpert, Holland) to investigate the crystal structure of Au and Ag nanoparticles. The measurement conditions were as follows: Target:CuKα, Wavelength = 1.5406 Å, Voltage = 40 kV, Current = 30 mA. The transmission electron microscope (TEM Model: Philips 300 nm) is used for determining size, shape and arrangement of the particles which make up the specimens. Figure (1) illustrates the PLAL method in NPs synthesis.

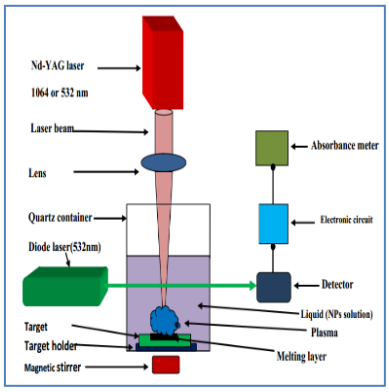

Fig. 1. A schematic diagram of PLAL method used in NPs synthesis.

The thin film deposition used in this work is called drop-casting method. This method is easy, simple, rapid technique, and yield a high volume of products with minimal waste. We use drop-casting method to prepare the surface of a thin film by dropping the solution onto a flat surface followed by evaporation of the solution. Figure (2) shows a diagram of thin film deposition using the drop casting method [17].

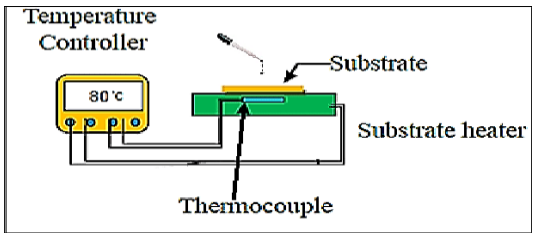

Fig. 2. A schematic diagram of thin film deposition by drop-casting method [17].

3. Result and Discussion

3.1. Structural and Morphological Characteristics of Nanoparticles

In this study, X-ray Diffraction (XRD) patterns and Transmission Electron Microscopy (TEM) were used to determine the crystalline size and the shape of the NPs, respectively.

3.1.1. X-ray Diffraction Results

X-ray diffraction patterns for all Au-NPs and Ag-NPs prepared with a power of 520 mJ and different laser pulses (150, 250, 350, 450, 550, 650) were obtained and analyzed. Crystallite size was calculated from the determination of full width half maximum (FWHM) and Miller indices by using Scherrer's equation:

$$D = \frac{K\lambda}{\beta \cos\theta} \tag{1}$$

where D corresponds to the crystallite size in Å.
$\lambda = 1.54059$ Å is the X-ray wavelength.
K: is a dimensionless shape factor, with a value of 0.9.
θ is the Bragg angle and β corresponds to the full width at half maximum (FWHM) in radians of the peak under consideration [18].

$$2d\sin\theta = n\lambda \tag{2}$$

where n is the order of diffraction pattern.

Lattice constant has been found using the formula:

$$a = d * \sqrt{(h^2 + k^2 + l^2)} \tag{3}$$

where (d) is the space between atomic plane in the crystalline phase, (a) is lattice constant, h, k, and l are Miller indices [19]. Bragg's Law was used to calculate the value of the interplanar spacing between the atoms. All values of (d) are obtained and given in tables (1) and (2). It is seen that the values are nearly the same. The results are in agreement with the literature [20].

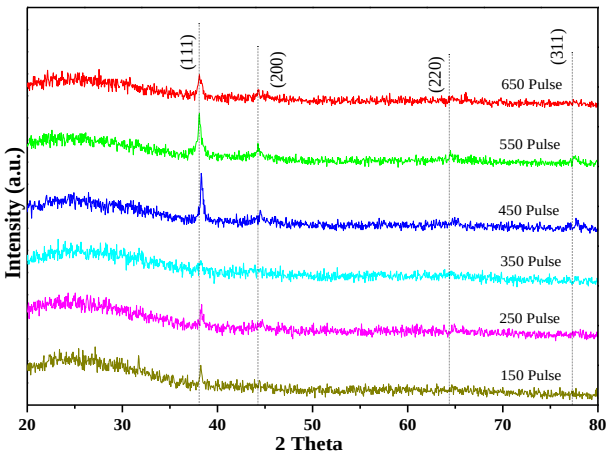

Fig. 3. X-ray diffraction patterns of gold nanoparticles using different numbers of pulses (150, 250, 350, 450, 550 and 650).

Figure (3) shows XRD patterns of the Au nanoparticles prepared on glass substrates at different numbers of pulses. The results exhibit the pure cubic crystalline structure at all the pulses used. The X-ray patterns of the prepared Au nanoparticles are precisely identical to the standard patterns (JCPDS 005-3763) , lattice parameters and angles (a = b = c = 4.0900 ˚A) ($\alpha = \beta = \gamma = 90°$) respectively. Four peaks can be observed at the angle 38.114, 44.287, 64.399 and 77.343

which correspond to the orientations (111), (200), (220) and (311) respectively. The result is in agreement with other reports [21,22]. Table (1) illustrates the agreement between experimental and standard data of gold nanoparticles.

Table 1. Experimental and standard results of X-ray diffraction of gold nanoparticles.

2Θ (deg) Experimental	2Θ (deg) Standard	FWHM (deg)	crystalline size "D" (nm)	d_{hkl} (Å) Experimental	d_{hkl} (Å) Standard	(hkl)	$h^2+k^2+l^2$	Lattice const.'a' (Å)
38.114	38.078	0.7571	9.91	2.3592	2.3613	(111)	3	4.086
44.287	44.256	0.7234	10.17	2.0436	2.0450	(200)	4	4.087
64.399	64.376	0.9502	7.07	1.4455	1.4460	(220)	8	4.088
77.343	77.312	0.6126	10.12	1.2327	1.2331	(311)	11	4.088

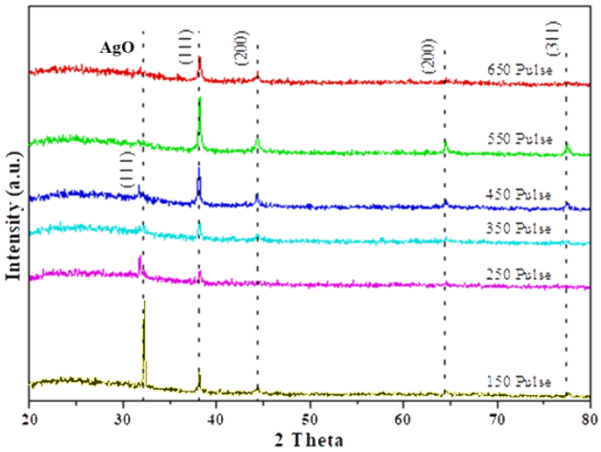

Fig. 4. X-ray diffraction patterns of silver nanoparticles at different number of pulses (150, 250, 350, 450, 550 and 650).

Figure (4) shows the X-ray diffraction (XRD) patterns of Ag nanoparticles prepared on glass substrate at different numbers of pulses, The X-ray diffraction patterns reveal that the silver particles have formed a pure cubic crystal structure are precisely identical to the standard patterns (JCPDS 89-3722), lattice parameters and angles (a = b = c. = 4.0855 Å), (α = β = γ = 90°), respectively. They also show the formation of another cubic crystal structure attributed to AgO particles identical to the standard patterns (JCPDS 03-5662), lattice parameters and angles (a = b = c = 4.8160 Å) (α = β = γ = 90°) respectively at (150, 250, 350 and 450) pulses. We observe four peaks at the angles 38.185, 44.353, 64.536, 77.470 which correspond to the orientations (111), (200), (220) and (311) respectively. In addition, we observed one peak at the angle 32.263 which corresponds to the orientations (111) attributed to AgO particles. Table (2) illustrates the agreement between experimental and standard data of silver nanoparticles.

Table 2. Experimental and standard results of X-ray diffraction of silver nanoparticles.

2Θ (deg) Experimental	2Θ (deg) Standard	FWHM (deg)	crystalline size "D" (nm)	d_{hkl} (Å) Experimental	d_{hkl} (Å) Standard	(hkl)	$h^2+k^2+l^2$	Lattice const.'a' (Å)
32.263 AgO	32.167	0.196	38.93	2.772	2.78	(111)	3	4.801
38.185	38.121	0.3182	23.59	2.354	2.358	(111)	3	4.077
44.353	44.307	0.7353	10	2.040	2.042	(200)	4	4.080
64.536	64.456	0.3275	20.51	1.442	1.444	(220)	8	4.078
77.470	77.414	0.2298	26.96	1.231	1.231	(311)	11	4.082

3.1.2. TEM studies of Au and Ag nanoparticles

TEM was used to examine gold and silver nanoparticles colloidal solutions synthesized by PLAL technique using different number of pulses (150, 250, 350, 450, 550 and 650). The lowest and highest (150 and 650) pulses are selected for each of the gold and silver samples as shown in Figures (5) and (6). Figure (5) shows TEM micrographs of Au-NPs. The nanoparticles are spherical in shape with (2.44-29.41 nm) and (2.79-36.61 nm) in diameter of size for two pulses (150 and 650), respectively. Both samples consisted of particles with a similar spherical shape and average size of (7.95 nm to 11.36 nm) as shown in the histogram.

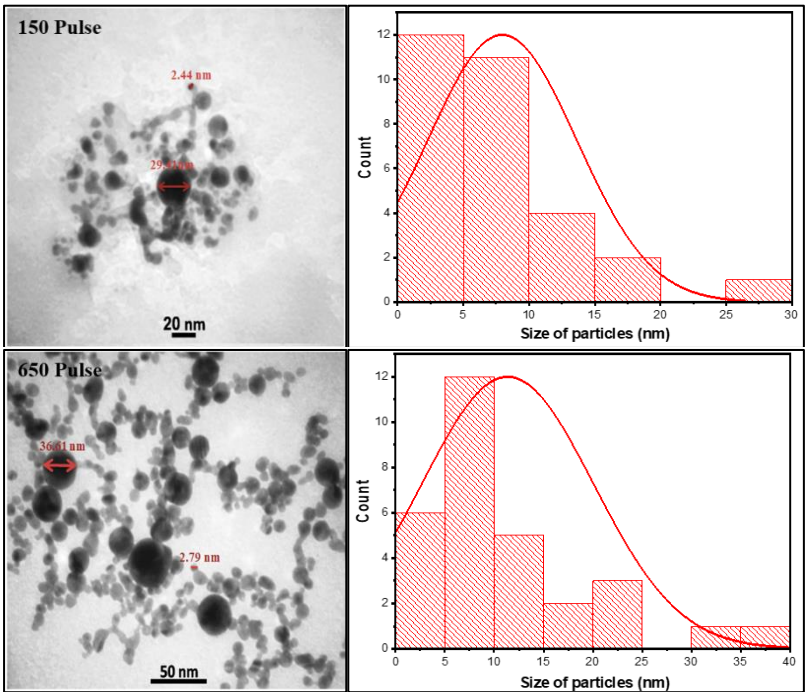

Fig. 5. TEM micrograph images correlated with size distributions of gold NPs at (150, 650) pulses.

Figure (6) shows semi-spherical shape of Ag-NPs with (3.06 nm to 46.51 nm) and (3.73 nm to 57.34 nm) diameter of size, for two pulses (150 and 650) and both samples consist of particles with a similar shape and average-sized of (15.62 to 20.49 nm) as shown in the histogram.

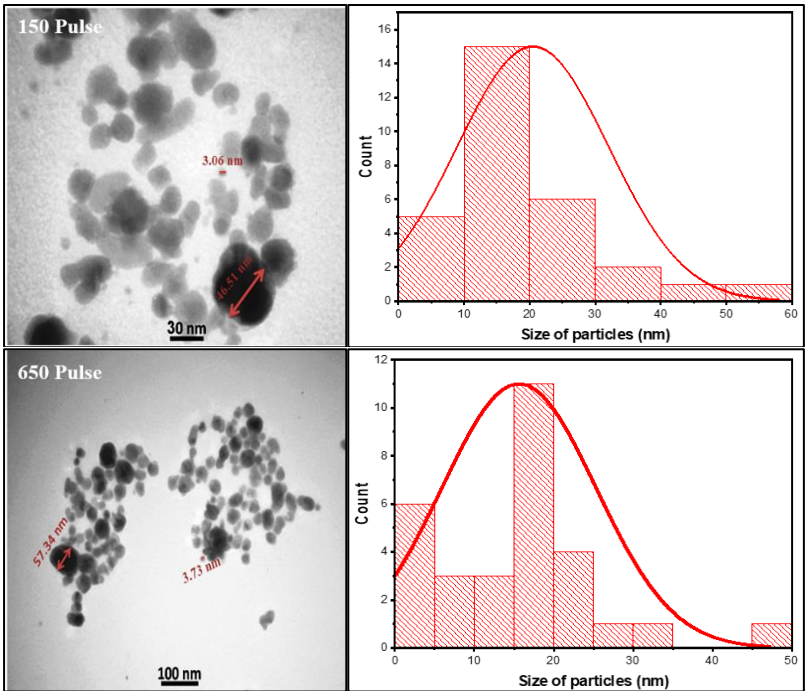

Fig. 6. TEM micrograph images correlated with size distributions of silver NPs at (150, 650) pulses.

3.2. Optical Properties of Au-Ag nanoparticles

NPs of gold and silver were made in distilled water at the wavelength between 532-1064 nm by using a Q-switched Nd:YAG-pulsed laser. A color change was occurred in gold colloidal solutions from faded to red, while with silver solution, the color became yellow. Figure (7) shows the color of gold and silver nanoparticles colloidal solutions synthesized by PLAL technique using different numbers of pulses (150, 250, 350, 450, 550 and 650).

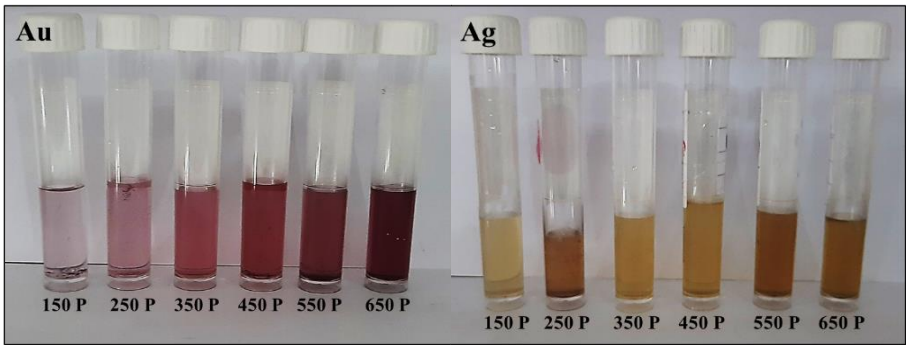

Fig. 7. Color of gold (Au) and silver (Ag) nanoparticles colloidal solutions using different numbers of pulses.

Figures (8) and (9) show the optical absorption spectra of gold and silver nanoparticles colloidal solutions synthesized by PLAL technique using different numbers of pulses (150, 250, 350, 450, 550 and 650). The optical absorption spectra were investigated in a wavelength range between 300-1000 nm by UV/Vis spectrophotometer. Gold and silver colloidal solutions showed strong SPR absorption bands at 520 nm and (404-410) nm, respectively. With the increase of laser pulses, the absorbance of gold NPs (0.139 – 0.908 arb.units) and silver NPs (0.612–2.212 arb.units) were increased as well. High laser pulses resulted in a high absorbance value, indicating that the solutions contain a high concentration of NPs. By increasing the number of pulses, the

optical absorption density of the liquid medium increased which indicates that the number of pulses had an impact on the density and number of nanoparticles [23].

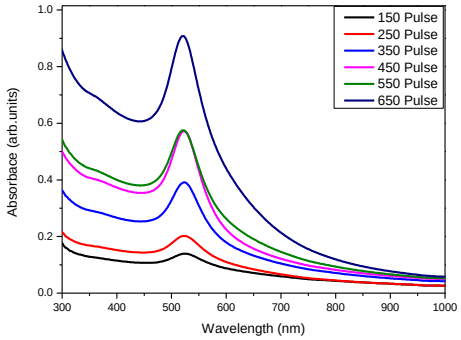

Fig. 8. UV–Vis absorption spectra of gold NPs synthesized by PLAL technique using different numbers of pulses (150, 250, 350, 450, 550 and 650).

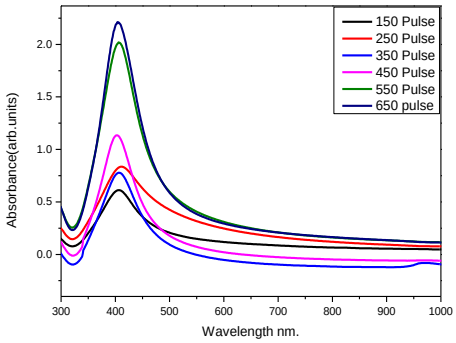

Fig. 9. UV–Vis absorption spectra of silver NPs synthesized by PLAL technique using different numbers of pulses (150, 250, 350, 450, 550 and 650).

4. Conclusion

This study investigated the effect of six different laser pulses on synthesis of Au-NPs and Ag-NPs in distilled water. The PLAL technique was used to examine the optical absorption spectra, colors and the average sizes of Au-NPs and Ag-NPs. The structures, optical properties, and morphology of synthesized NPs were investigated using a variety of measurements. X-ray diffraction (XRD) patterns of the Au-NPs and Ag-NPs prepared on glass substrates at different numbers of pulses exhibit pure cubic crystalline structure. The absorbance of gold NPs and silver NPs was increased as the laser pulses were increased. High laser pulses resulted in a high absorbance value, indicating that the solutions contain a high concentration of NPs. The TEM examination shows spherical shapes of Au-NPs and semi-spherical shapes of Ag-NPs. With increasing laser pulses, the average size of Au and Ag increased.

Acknowledgements

The authors would like to thank the University of Diyala/College of Science/Department of Physics for the technical support to complete this work in their laboratories.

References

[1] P. Sen, J. Ghosh, A. Abdullah, P. Kumar, Vandana, Proc. Indian Acad. Sci. (Chem. Sci.) **115**, 499 (2003).
[2] D. Mahl, J. Diendorf, S. Risting, C. Greulich, Zi-An Li, M. Farle, M. Koller, M. Epple, J Nanopart Res **14**(1153), 1 (2012).
[3] A.Voloshko, T. E. Itina, Nanoparticles Technology, 1 (2015).
[4] I. A. Abdul-Hassan, I. M. Ibrahim, Z. S. Shalla **8**(49), (2018).
[5] H. Zeng, W. Cai, Y. Li., J. Hu, P. Liu, The Journal of Physical Chemistry **109**(39), 18260 (2005).
[6] H . Huang, J. Lai, J. Lu, Z. Li, AIP Advances **9**, 015307 (2019).
[7] J. Perrière, E. Millon, E. Fogarassy, Recent advances in laser processing of materials, Elsevier, Publication Oxford, United Kingdom, 1st Edition, 472 (2006).
[8] R. G. Khadim, M. F. Noori, A. K. Ali, Journal of Babylon Univ. Pure Appl. Sci. **22**(1), 547 (2012).
[9] W. Norsyuhada, W . Shukri, N . Bidin, S. Islam, G. Krishnan, M. A. Abu Bakar, M. S. Affandi, Journal of Nanophotonic **10**(4), 046007 (2016).
[10] W. Norsyuhada, W. Mohd Shukri, H. Bakhtiar, S. Islam, N. Bidin, International Journal of Nanoscience **17**(3), 1850015 (2018).
[11] V. A. G. Rivera, F. A. Ferri, E. Marega Jr, Plasmonics-Principles and Applications, 283, ch. 11, (2012).
[12] C. Dhand, N. Dwivedi, X. J. Loh, A. N. J.Ying, N. K. Verma, R. W. Beuerman, R. Lakshminarayanan, S. Ramakrishna, Rsc Advances **5**(127), 105003 (2015).
[13] A. Fojtik, A. Henglein, Phys. Chem. **97**, 252 (1993).
[14] N. Hia, Z. Li, Z. J.-Ying, Z. Mi-Lin, B. Xu-Duo, Optoelectronics Letters **6**(2), 81 (2010).
[15] M. J. Haider, M. S. Mehdi, Engineering and Technology Journal Part B **32**(4), 704 (2014).
[16] T. Tsuji, Laser ablation in liquids, Principles and Applications in the Preparations of Nanomaterials, ed. G. Yang (Pan-Stanford Publishing, Singapore, (2012).
[17] A. N. Abd, D. M. A. Latif, W. M. Abdulridha, Journal of Multidisciplinary Engineering Science Studies (JMESS) **2**, 2458 (2016).
[18] Z. T. Khodair, N. A. Bakr, A. M. Hassan, A. A. Kamil, Journal of Ovonic Research **15**(6), 377 (2019).
[19] Z. T.Khodair, A. A. Kamil, Y. K. Abdalaah, Physica B **503**, 55 (2016).
[20] B. K. Mehta, Meenal Chhajlani, B. D. Shrivastava, IOP Conf. Series: Journal of Physics: Conf. Series **836**(1), 012050 (2017).
[21] I. A. Hameed, M.Sc. Thesis, College of Science, University of Diyala, (2019).
[22] F. A. H Mutlak, M. Jaber, H. Emad, Iraqi Journal of Science **58**(4C), 2364 (2017).
[23] A. A. Salim, N. Bidin, H. Bakhtiar, S. K. Ghoshal, M. Al Azawi, G. Krishnan, Journal of Physics: Conference Series **1027**(1), 012002 (2018).